Cell Prolif. 2007, **40**, 268–281

Identification of stathmin 1 expression induced by Epstein–Barr virus in human B lymphocytes

S. Y. Baik*, H. S. Yun*, H. J. Lee*, M. H. Lee*, S. E. Jung*, J. W. Kim*, J. P. Jeon*, Y. K. Shin†, H. S. Rhee‡, K. C. Kimm* and B. G. Han*

**Biobank for Health Sciences, Center for Genome Sciences, National Institute of Health, Korea Center for Disease Control and Prevention, Seoul, South Korea, †Chungbuk Bio Industry Foundation Health Industry Center, Chungbuk, South Korea, ‡Department of Clinical Genetics, Yonsei University College of Medicine, Seoul, South Korea*

Received 23 *August* 2006*; revision accepted* 23 *November* 2006

Abstract. *Introduction*: The Epstein–Barr virus transforms resting B cells into proliferating lymphoblastoid cells, the origin of cell lines. *Method and results*: Our cDNA microarray analyses led to the identification of 232 up-regulated and 112 down-regulated genes with more than a 3-fold difference in lymphoblastoid cell lines compared to resting B cells. The functional classification of these genes exhibited the distinct expression signature for cell proliferation, cell cycle and an immune response. Among them, we verified the differential expression of several oncogenes such as *stathmin 1* (*STMN1*), *RAB27A*, *RAB9A*, *BACH1* and *BACH2* using quantitative real-time reverse transcriptase-polymerase chain reactions or Western blot analysis. Expression of *STMN1* (which is involved in regulation of the microtubule filament system, cell growth and S-phase of cell cycle) was increased in lymphoblastoid cell line as well as in 7-day post-Epstein–Barr virus infection B cells, compared to resting B cells. *Conclusion*: Thus, this study suggests that Epstein–Barr virus infection induces *STMN1* expression, which play a role in cell cycle progression and proliferation in the human B lymphocyte.

INTRODUCTION

The Epstein–Barr virus (EBV) is a member of a human herpevirus subfamily that establishes life-long persistent infection in over 90% of the human adult population worldwide. The virus can be isolated from cultured Burkitt lymphoma (BL) cells. Although EBV infection is not generally related to cancer development, it is well known to be linked to several specific human cancers such as Burkitt's lymphoma, nasopharyngeal carcinoma and some types of gastric cancers. In addition, EBV usually causes lymphoid proliferation resulting in lymphoma in immunocompromised patients (Al Saati *et al*. 1992; Tsurumi *et al*. 2005). Based on its association with this variety of lymphoid and epithelial malignances, EBV has been classified as a group 1 carcinogen by the International Agency for Research on Cancer. Specifically, EBV *in vitro* infects resting B lymphocytes via

Correspondence: Dr. B. G. Han, Biobank for Health Sciences, Center for Genome, Science, National Institute of Health, Nokbun 5, Eunpyung-Gu, Seoul 122-701, South Korea. Tel.: +82 2 380 2258; Fax: +82 2 354 1078; E-mail: bokghee@yahoo.com

CD21 and human leucocyte antigen (HLA) class II molecules on the cell surface, inducing continuous proliferation of the infected B cells (Tsurumi *et al*. 2005). As a result, resting B lymphocytes have been transformed *in vitro* into proliferating lymphoblastoid cell lines (LCL) by EBV infection. LCLs have been used widely for various purposes: in aetiological studies of tumorigenesis by EBV; for studies of immunology and cellular biology and as sources of DNA and cells to study various genetic disorders (Sugimoto *et al*. 2004). Because LCLs proliferate, genome sources isolated from LCLs can be provided stably for researchers. The LCLs express a limited number of EBV gene products, including six nuclear proteins (EBNA-1, EBNA-2, EBNA-3A, EBNA-3B, EBNA-3C and EBNA-LP), integral latent membrane proteins (LMP-1, LMP-2A and LMP-2B), the BamA right transcript (BART) and two small RNAs (EBER). Among these, EBNA-1, EBNA-2 and LMP-1 seem to be required constitutively for EBV-transformed LCLs (Bornkamm & Hammerschmidt 2001). These proliferating LCLs change into an immortalized, tumourous LCL by genes of host cells in cooperation with EBV genes (Sugimoto *et al*. 2004).

It is necessary to understand the biological characteristics of LCLs more fully as they have been widely used as resources for a variety of immunological and genetic studies. Thus, we have attempted to identify their biological characteristics through comparing the profiles of gene expression between LCLs and resting B cells. Previous comparisons between the EBV-infected BL and BL with a c-Myc translocation and p53 mutations (Cohen *et al*. 1987; Farrell *et al*. 1991) did not identify the genes whose expression changed at various points in the cell cycle and proliferation (Carter *et al*. 2002). However, in our study, comparisons between resting B cells and the corresponding LCL enabled the identification of genes whose expression changed during the cell cycle and thus proliferation.

MATERIALS AND METHODS

Preparation of infectious EBV stocks

Epstein–Barr virus stocks were prepared from an EBV-transformed B95-8 marmoset cell line. The cells were grown in an RPMI-1640 medium (Gibco/BRL, Gaithersburg, MD, USA) supplemented with 10% foetal bovine serum (Bio Whittaker, Walkersville, MD, USA) for 7–10 days until the medium turned yellow and the cells were 90% confluent. Culture supernatants were then harvested for infectious EBV stocks, and were stored at −80 °C until needed.

Purification of resting B cells and EBV infection

Ten volunteers participated in this study, and informed consent was obtained from all participants. Sixty millilitres of peripheral blood was collected in a syringe containing heparin. Peripheral blood mononuclear cells (PBMC) were isolated from the whole blood by Ficoll Hypaque gradient centrifugation (Amersham Bioscience, Uppsala, Sweden). B cells were purified (> 95% CD20+) using a B-cell isolation kit and MACS separators (Miltenyi Biotec, Auburn, CA, USA). The purified resting B cells were infected with EBV by adding the B95-8 supernatant in a culture flask (Neitzel 1986). Following 2-h incubation at 37 °C, the same volume of complete medium containing cyclosporin A (0.5 μg/ml) was added (Pelloquin *et al*. 1986). Cultures were incubated for 4 weeks until clumps of EBV-infected B cells were visible and the medium turned yellow. As a result, the resting B cells were efficiently transformed into permanently growing cells called LCLs. In this experiment, we purified 10 resting B cells and established 10 LCLs from 10 normal donors.

Reverse transcriptase-polymerase chain reaction for EBV-encoded gene expression

Total RNAs were prepared from resting B cells and LCLs using TRIzol according to the manufacturer's instructions (Invitrogen, Carlsbad, CA, USA). Reverse transcription was carried out using 1 μg of total RNA isolated from the resting B cells or LCLs. We performed reverse transcriptase-polymerase chain reaction (RT-PCR) to confirm the expression of EBV-encoded genes. *LMP1*, *EBNA2* and *EBNA3A* genes were included in the RT-PCR. Among them, *EBNA2* and *EBNA3A* were used as markers for a latency III infection of EBV. The primer sequences of *LMP1* are forward 5′-CCTCAACAAGCTACCGATGA-3′ and reverse 5′-ACCTCTTCCGTCAATTCTGG-3′. Primer sequences of *EBNA-2* are forward 5′-CTCGCCACCTGCAACACTA-3′ and reverse 5′-AGAGGGTGCATTGATTGGTC-3′. Primer sequences of *EBNA3A* are forward 5′-ACATGAACAACACGGCATGG-3′ and reverse 5′-TGATGTTGGGCCACGTCAGT-3′. Primer sequences of glyseraldehyde-3-phosphate dehydrogenase (GAPDH) are forward 5′-CAGGGCTGCTTTTAACTCTGGTAA-3′ and reverse 5-GTGGAATCATATTGGAACATGTAAACC-3′. The PCR products were visualized on a 1% agarose gel.

Preparation of total RNA and microarray analysis

For microarray analysis, we used six GeneTrack® (Seoul, Korea) Human cDNA 17K chips containing the known genes, 11 135 and several control genes such as *GAPDH*, *beta-actin* and *alpha-tublin* (Genomictree). Total RNA was prepared from six resting B cells and LCLs. For preparation of the cDNA probe, 50 μg of total RNA was used and converted to cDNA by reverse transcriptase using oligo(dT) (Invitrogen). The cDNA probe for resting B cells that was used as a control was labelled with Cy3-dUTP, while each corresponding LCL that was used as a test was labelled with Cy5-dUTP. The Cy3- and the Cy5-labelled probes were combined into a reaction mixture. Labelled cDNA probes were then purified by a QIAquick PCR purification kit (Qiagen, Hilden, Germany). After purification the probe solution was concentrated to make a hybridization mixture using microcon-30 (Millipore, Bedford, MA, USA), until the appropriate volumes of probe solutions were reached. After denaturation of the hybridization mixture containing the probe solution, we mixed well and applied the mixture carefully between the DNA chip slide and cover slip. After hybridization, the microarray plate was washed and dried. The array was then scanned with an Axon scanner 4000B. The experimental data from the microarray analysis was normalized by LOWESS normalization. Total microarray experiments were then replicated six times. The correlation coefficient between six replicates was 0.93, indicating sufficient reproducibility. We analysed the microarray data using Genplex™ program (ISTECH, Seoul, Korea). This is a commercial program for analysis and visualization of the results of complex microarray experiments. Biologically relevant groups from the microarray data were generated using both the Netaffx from Affymetrix (Santa Clara, CA, USA) and the Database for Annotation, Visualization and Integrated Discovery (DAVID; version 2.1) from the National Institutes of Allergy and Infectious Disease.

Real-time RT-PCR

Total RNAs were prepared from six resting B cells or their corresponding LCLs. Real-time RT-PCR was performed using an ABI PRISM 7900HT Sequence Detection System (Applied Biosystems, Foster City, CA, USA). The reaction mixture for the SYBR Green assay contained 2×SYBR Green PCR Master Mix (Applied Biosystems), 10 pmol of the forward and reverse primers, and cDNA. All the amplifications and detections were carried out in a 384-well reaction plate with optical caps and a MicroAmp Optical 384-Well Reaction Plate (Applied Biosystems). At each cycle, the accumulation of PCR products was detected by monitoring the increase in the fluorescence of reporter dye from the dsDNA-binding SYBR Green. Following the real-time

Table 1. Oligonucleotide sequence of primers used in the real-time reverse transcriptase-polymerase chain reaction

Gene symbol		Oligonucleotide sequences
STMN1	Forward	5′-GCCAGGCTTTTGAGCTGATTC-3′
	Reverse	5′-CATGGGACTTGCGTCTTTCTTC-3′
RAB27A	Forward	5′-ACAAACATAAGCCAAGCAATTGAGA-3′
	Reverse	5′-CCTTCAGGAATCCAGGACTTGTC-3′
RAB9A	Forward	5′-TGGAGATGGTGGAGTTGGGA-3′
	Reverse	5′-CTATTGTATGGAAGAGCTGGGTATCAA-3′
BACH1	Forward	5′-TTCACCTGAGAATTCACCGTAACA-3′
	Reverse	5′-GATACAGGTTGCATGTGGACACTC-3′
BACH2	Forward	5′-TGGCCTGCCCAGTACATCTC-3′
	Reverse	5′-AAGGTCACCCTGAGTGATCCC-3′
GAPDH	Forward	5′-CAGGGCTGCTTTTAACTCTGGTAA-3′
	Reverse	5′-GTGGAATCATATTGGAACATGTAAACC-3′

RT-PCR, a dissociation curve (melting curve) between 60 °C and 95 °C was generated during a temperature ramp. A gene encoded glyceraldehyde-3-phosphate dehydrogenase (GAPDH) was used as an internal control. All data were analysed using the relative standard method. In brief, the each quantity of the target or *gapdh* gene was calculated from its standard curve. Level of the target gene's expression was normalized against the level of the *gapdh* gene expression. Oligonucleotide sequences of the primers used in this study are shown in Table 1. For the design of all the primers, Primer Express 2.0 was used (Applied Biosystems).

Western blot analysis

Total proteins were prepared from four resting B cells and four of their corresponding LCLs. Three independent Western blot analyses were performed as previously described. Cell pellets were washed with ice-cold 1 × phosphate-buffered saline and were sonicated in 200 μl of Radioimmunoprecipitation assay buffer (150 mM NaCl, 10 mM Tris-HCl, pH 7.2, 1% sodium deoxycholate, 0.1% sodium dodecyl sulphate [SDS], 2 μg/ml aprotinin, 1 mM EGTA, 1 mM PMSF and 1 mM sodium orthovanadate) with an ultrasonic processor, for 3 s on ice. After centrifugation for 10 min at 10 000 × ***g*** at 4 °C, supernatants were obtained and a modified Bradford protein assay was performed with the supernatants (Bio-Rad, Hercules, CA, USA). Thirty micrograms among the total proteins were fractionated on 15% SDS-polyacrylamide gel electrophoresis (PAGE) and were transferred by electroblotting onto the polyvinylidene difluoride. A Western blot analysis was performed by incubating polyvinylidene difluoride with a rabbit polyclonal stathmin 1 (STMN1) antibody diluted to 1 : 1000 in a blocking buffer overnight at 4 °C (Calbiochem, San Diego, CA, USA). Immunoreactive bands were identified with horseradish peroxidase-conjugated secondary antibodies diluted to 1 : 2000 in a rinsing buffer for 1 h. We used the enhanced chemiluminescence developing kit (PerkinElmer Life Sciences, Boston, MA, USA). Such antigen–antibody complexes show the chemiluminescent signal captured on X-ray film.

Cell proliferation assay

Resting B cells were infected with EBV by adding the B95-8 supernatant in a culture flask (Neitzel 1986). Following 2 h incubation at 37 °C, the same volume of complete medium containing cyclosporin A (0.5 μg/ml) was added (Pelloquin *et al*. 1986). The cultures (1×10^5) were incubated for 1 or 7 days. Cell proliferation was measured using the CellTiter 96® Non-Radioactive

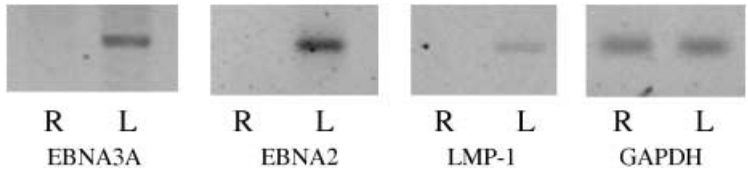

Figure 1. Confirmation of EBV-transformed LCL by the expression of EBV-latency genes. Resting B cells are primary B cells freshly isolated from human blood. The cells were incubated with EBV (B95-8) stock supernatant for 2 h and then were cultured for 4 week, to LCL. We confirmed the expression of EBV latency III genes in the EBV-transformed LCL by RT-PCR. *EBNA-3A*, *EBNA-2* and *LMP-1* are the latency III EBV-encoded genes. GAPDH was used as an internal control. R, Resting B cell; L, LCL.

Cell Proliferation Assay (Promega, Madison, WI, USA) according to the manufacturer's instructions. The cells were incubated for 4 h at 37 °C with dye solution containing a tetrazolium component. During a 4-h incubation, living cells convert the tetrazolium component of the dye solution into a formazan product. After 4 h incubation, we added a stop solution, incubated for 1 h, and then mixed using multi-channel pipet. The absorbance at 570 nm was recorded using a 96-well plate reader.

Flow cytometric analyses

Propidium iodide (PI) staining of cells was performed for cell cycle analyses. Resting B cells were infected with EBV and were cultured for 1 or 7 days. For the PI staining, we used a CycleTEST™ PLUS DNA Reagent Kit (Becton Dickinson Biosciences, San Jose, CA, USA). After centrifugation of cell suspensions at $400 \times \boldsymbol{g}$ for 5 min, 250 µl of solution A (trypsin buffer) was added to each tube. After incubation for 10 min at room temperature, 200 µl of solution B (trypsin inhibitor and RNase buffer) was added to each tube. After incubation for 10 min, 200 µl of cold solution C (PI stain solution) was added to each tube. After incubation for 10 min in the dark on ice, the samples were analysed within 3 h using a Becton Dickinson FACS Canto™ flow cytometer at 488 nm single laser excitation. The cell cycle distribution was determined using ModFit *LT*™ software.

RESULTS

LCL establishment and EBV gene expression

We isolated 10 resting B cells from human peripheral blood and then established each corresponding LCL for the 10 resting B cells. These LCLs were verified to express the EBV-encoded genes *LMP1*, *EBNA2* and *EBNA3A* by RT-PCR (Fig. 1). The resting B cells did not express the EBV-encoded genes, indicating that they were EBV-negative with respect to EBV gene expression. The LCLs used in our study also were latency III infection as they showed latency III characteristics of the expression of *EBNA2* and *EBNA3A*.

Microarray analysis

To investigate gene expression profiles of LCLs and resting B cells, we used GeneTrack® Human cDNA 17K chips. Microarray analyses were performed six times from six resting B cells and the corresponding LCLs for biological replication. In total, 343 genes were selected as being

Table 2. The list of genes that were found to be significantly up-regulated in human lymphoblastoid cell lines

Functional group	Gene symbol
Transcription	STAT1, HNRPAB, PAR5, LOC51659, SNRPF, XPOT, NR0B2, PLAGL2, ZNF200, LMO2, CPSF5, TRIP6, CGI-94, H2AFZ, MSC
Apoptosis and cell death	CASP6, CFLAR, DAD1, PAK1, TNFRSF8, TNFAIP3, TNFRSF17, BID, PDCD5
Cell survival and proliferation	HSPA1L, RAB9A, RAB27A, MYBL2, HSPA1A, PCNA, PA2G4, HSPE1, HSBP1, SLC2A5, HSPCB, ATP5J, EMS1, AHSA1, ATP5J2, OC90410, ATP1A1, TRAP1, PRDX1
Cell cycle	CDK2, STMN1, CDC2, STK6, CCNA2, CCNG1, CDK4, CINP, PRC1, YWHAG, ACTB
Interferon and immune response	MX1, G1P2, IFI30, IFITM1, IFI35, IRF7, IGSF3, IGHM, CD59, BST2, CD38
Adhesion and signal transduction	CD58, PLEK, NK4, BASP1, LGALS1, RGS10, DBI, ITM2A, RACGAP1, NME1, VDAC3, SNX15, PTTG1, NME2, VDAC2, STK24, LLT4, CCL3, CCL18
Proteolysis and proteosome	DPP3, CPO, PSMD14, PSMA2, PSMA5, PSME2, PSMA3, PSMF1
Mitochondrion and electron transport	ATP5J2, IDH2, MRPL17, MTRF1, MTCH2, MRPS16, MDH2, PRDX3, FH, GLRX, ETFA, CYCS, COX8, COX6B, COX5A, CYC1, OX6C
Glycolysis	ENO1, LDHA, LDHB, ENO2
Cellular metabolism	MAPK6, PFKM, IREB2, TUBB2, HRI, CMAS, CCT8, DSS1, MOV10, GBE1, PMVK, GPI, CLN2, PCBD, GM2A, HMGA1, TPI1, WRN, CCT3, CCT5, LGALS3, OAS1, GARS, GRHPR, GATM, MTHFD2, SCD, PPIA, SDHC, HPRT1, GGTLA1, NDUFB6, NDUFS8, AHCY, ACADM, GOT2, NDUFAB1, PSAT1, FACL2, ATPIF1, CDIPT, GSTZ1
Carbohydrate metabolism	ALDOB, FUT1, ALDOA, PGD, ALDOC
Glycoprotein	PBEF, TPBG, CCL3, ADCY3, GENX-3414, CHI3L2, BSG, SLAM, PRG1, ADA, OAS1, DNAM-1
Protein transport	AP3B1, NAPA, CLTC, SEC23B, LMAN1, SEC24D, CLTB, KDELR2, SEC61G, KPNA3
Protein folding and synthesis	TCP1, PARK7, HKE2, CANX, SUI1, EIF2S2, WARS, SARS, RPS28, AARS, SSR3, SSR4
Other groups	CRACC, DC2, SNAP25, MLP, KCNN3, T2 BP, QP-C, HAPIP, STOML2, VMP1, FABP5, BIGM103, DMD, LRPPRC, TRIP10, MAD2L1, HDLBP, RCL, TKT, ACTG2, RRM2, METTL1, GGH, GPX1, TOP2A, PP, PHP14, COMT, APOBEC3B, ELL2, TOP2A, ENTPD1, PAICS, GSTP1, BIC, DXYS155E, H2-ALPHA, FDPS

The 232 up-regulated genes were classified into 15 functional groups. The functional groups are shown in Fig. 2. The fold ratio shows mean of the six microarray analysis results.

differentially expressed in LCLs according to the criteria of 3-fold difference of expression level. Among these, 232 genes were up-regulated and 111 genes were down-regulated in LCL (Tables 2 and 3). Most were newly identified as differentially expressed genes in LCLs except for those that had previously been reported (Carter *et al*. 2002). The result of hierarchical clustering for six microarray experiments was visualized by Genplex™ program (data not shown). Differentially expressed genes were categorized into 17 functional groups according to the principle functions of each gene (Tables 2 and 3). Functional classification represented a distinct expression profile in LCLs in which the genes involved in transcription and cellular metabolism, containing protein and carbohydrate, were most changed during EBV-mediated B-cell transformation (Fig. 2). Cell proliferation, immune response-related genes and cell cycles

Table 3. The list of genes that were found to be significantly down-regulated in human lymphoblastoid cell lines

Functional group	Gene symbol
Regulation of transcription	CIRBP, MYT1, BACH1, BACH2, TCF4, ATF7IP, DSIPI, LKAP, HRB2, YT521, PRDM2, FOXO1A, TRA2A, FLI1, MLL5, TLE1, H3F3A, RBM6
Apoptosis and cell death	LTB, TP53INP1, TUCAN, NKTR, MOAP1, DEFCAP
Cell survival and proliferation	RAB37, JUNB, VAV3, ATP6V1G1, BTG1, SLC15A2, TGFBR2
Cell cycle	DUSP1, CLK1, CCNL1
Immune response and interleukin	MS4A1, FCGR2A, CD83, HLA-DRB3, HLA-DMB, CD72, CD69, CD6, CD37, TCL1A, TAGAP, IL4R, IL2RA, IL16, IL10RA, ITGA4
Adhesion and signal transduction	SELL, NOTCH2, T, SH3BP5, RASGRP1, PDE4B, NR3C1, ITPR1, AKAP8, PTPRC, ADAM19, STK4, GABBR1, RGS2, ADAM28, DEFCAP
Proteolysis	CAPN2, SPPL2B
Mitochondrion	SLC9A6
B-cell-related factor	EBF, BCNP1, BCL9
Glycoprotein	CDW52, SMBP, CXCR4, TSPAN-3, DAF, TEAD2, CMG2
Cytoskeleton	ABLIM1, BICD2, ADD3
Protein metabolism	TRB2, PRKCB1, HERC3, SNARK, RNF141, BACE2
Other groups	ITSN2, DKFZP564B0769, UNC84B, MBNL2, SDCBP, PKIG, C3ORF6, RNPC1, NOD3, C13ORF9, SLA, OSBPL8, SYCP3, SNX2, OP1, DAPP1, DCK, DGKD, EBI2, MAP4K4, PRKCN, ZFHX1B, MGC17330

The 111 down-regulated genes were classified into 13 functional groups. The functional groups are shown in Fig. 2. The fold ratio shows the mean of six microarray analysis results.

associated genes were the next most changed functional groups (Fig. 2). Because LCLs were already known to have very high proliferation activity compared to resting B cells (Bornkamm & Hammerschmidt 2001), genes seen to be changed in this study were involved in cell survival, proliferation and cell cycle progression may play roles in the proliferation capacity of LCLs (Fig. 2). Thus, the LCL signature of the gene expression profile could be defined as a being of high proliferational activity, accompanying high metabolic activity, immune response potential and signal transduction.

Validation of microarray results

According to the results of the microarray analysis, 343 genes were differentially expressed between resting B cells and LCLs. We confirmed the expression of five genes at resting B cell and LCLs using real-time RT-PCR (Fig. 3a). Four oncogenes, *STMN1*, *RAB9A*, *RAB27A* and *MYBL2* were up-regulated, while three oncogenes, *RAB37*, *JUNB* and *VAV3* were found to be down-regulated in the LCLs by microarray analysis. Among them, we observed the expression level of three oncogenes, *STMN1* (stathmin 1/oncoprotein 18), *RAB27A* (member RAS oncogene family) and *RAB9A* (member RAS oncogene family), as abnormal over-expression of oncogenes such as *RAB1A* have previously been observed in many cancer cells (Shimada *et al*. 2005). We also investigated the expression level of an EBV integration related gene, *BACH2* and its family member, *BACH1*, as loss of *BACH2* has been observed by integration of EBV into the human genome in a Burkitt lymphoma cell line (Takakuwa *et al*. 2004). It was revealed that the fold change of *STMN1* expression was 5.5 ± 1.4 ($P = 0.000$) in LCLs by microarray analysis and 1.87 ± 0.27 ($P = 0.001$) fold in LCLs by real-time RT-PCR (Fig. 3a). *RAB27A* and *RAB9A* genes showed multiplication of 6.6 ± 1.9 ($P = 0.000$) fold and 5.7 ± 1.9 ($P = 0.000$), respectively, in LCLs by microarray analysis and 1.69 ± 0.07 ($P = 0.002$) and 2.04 ± 0.42 ($P = 0.01$)

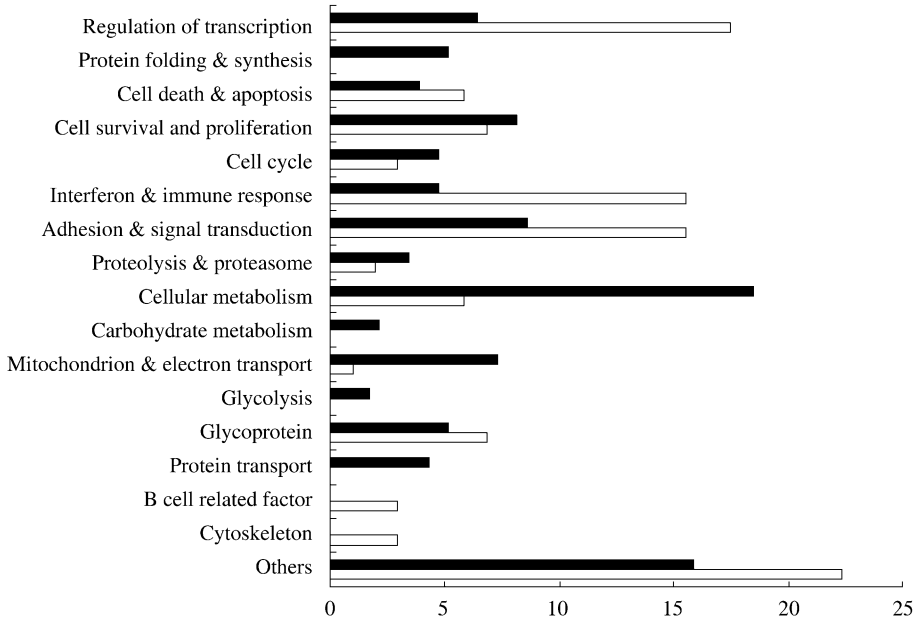

Figure 2. Functional classification of microarray data. Classification of the up-regulated or down-regulated genes according to functional groups. A total of 343 changed genes were classified into 17 functional groups by the analyses of Gene Ontology on based on DAVID/Netaffx. The black bar represents functional groups of up-regulated genes. On the other hand, the white bar represents functional groups of the down-regulated genes.

fold in LCLs by real-time RT-PCR (Fig. 3a). *BACH1* and *BACH2* were present only 0.2 ($P = 0.000$) fold in LCLs by microarray analysis and each was 0.03 ($P = 0.000$) and 0.0001 ($P = 0.000$) fold increase in LCLs by real-time RT-PCR (Fig. 3a). mRNA levels encoded by five genes tested here showed consistent up- or down-regulation observed by microarray data although absolute expression level of each gene by real-time RT-PCR was found to be different from data provided by the microarray analysis.

We performed Western blot analysis to confirm the STMN1 protein level in resting B cells and LCLs. STMN1 was shown as a doublet with the upper band significantly increased in LCLs and the lower band somewhat increased in resting B cells. Total intensity of the STMN1, shown as a doublet, was weaker in resting B cells than in LCL (Fig. 3b). It has also been previously reported that the lower molecular weight band was the result of the proteolytic cleavage of the N-terminus of the protein (Koppel *et al*. 1990). Because this anti-STMN1 analysis detects the C-terminus of the molecule, the upper band presents intact STMN1, whereas the lower band presents a degraded STMN1. Thus, it is speculated that intact STMN1 is increased significantly in the LCLs compared to the appropriate resting B cells. In this study, beta-actin was included as a loading control (Fig. 3b). Thus, we conclude that *STMN1* gene expression is up-regulated in LCLs at both transcriptional and translational levels.

Identification of STMN1 expression in EBV-infected B cells

In this study, we identified increases of STMN1 mRNA or protein expression in LCL. To identify STMN1's role in EBV-induced transformation, the level of STMN1 mRNA was analysed by real-time RT-PCR in resting B cells and 1 or 7 days post-EBV infection. The increase of

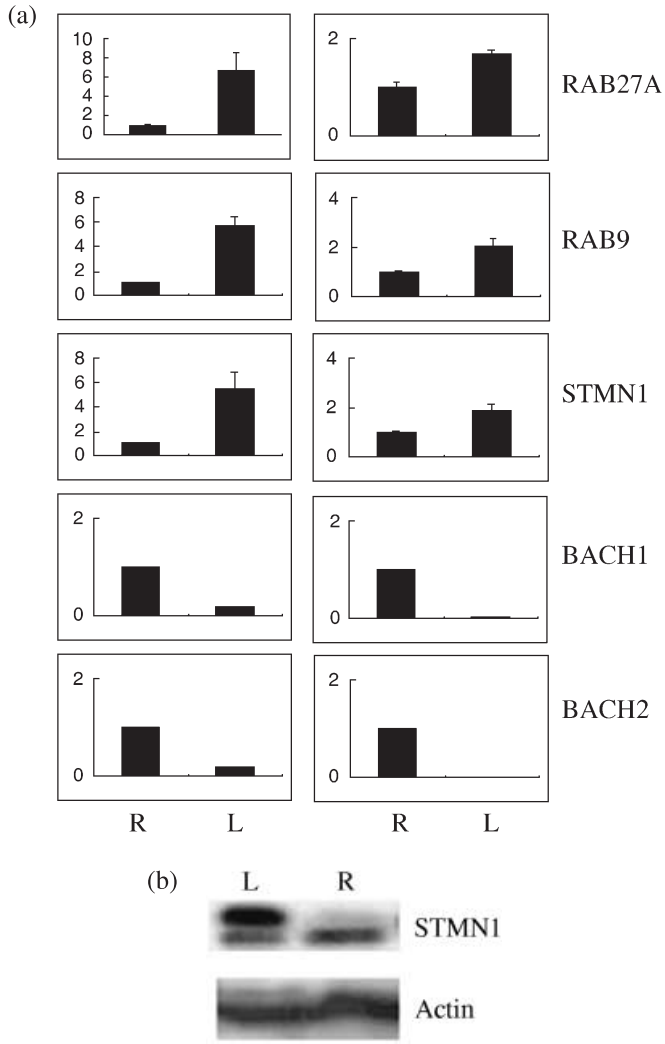

Figure 3. Validation of microarray results. We performed real-time RT-PCR to confirm the expression of genes changed in LCL through microarray analysis (a). The results of the real-time RT-PCR were analysed according to the relative standard method. Expression level of a target gene was normalized as in resting B cells and the LCL with the expression level of an internal control, GAPDH. Target genes are *RAB27A*, *RAB9A*, *STMN1*, *BACH1* and *BACH2*. Statistical analysis was performed with a paired two sample *t*-test using SPSS 12.01 ($P < 0.05$). We performed Western blot analysis to confirm protein expression of *STMN1*, changed in LCL, by microarray analysis (b). We loaded each 30 μg of total protein for resting B cells and LCL in 15% SDS-PAGE gel. Anti-STMN1 was used as the primary antibody. We used anti-β-actin antibody as an internal control. The STMN1 protein showed at 17–18 kDa, β-actin at 42 kDa. The upper band presents an intact STMN1, whereas the lower band presents a degraded STMN1. This is representative data from four different experiments. L, LCL; R, Resting B cell.

STMN1 mRNA was observed and not in resting B cells or the day 1 post-EBV infection cohort, but was detected in the 7-day post-infection cells (Fig. 4). According to the above results, STMN1 mRNA was up-regulated in LCL and in 7-day post-EBV infected cells compare to resting B cells (Figs 3 and 4).

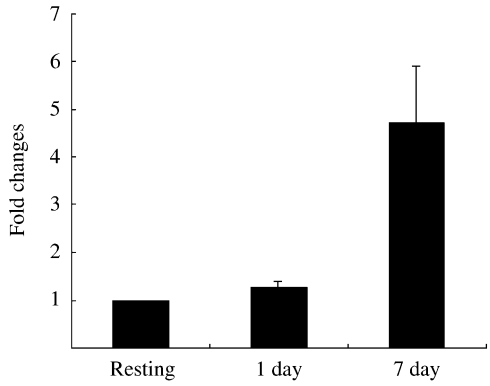

Figure 4. Change of STMN1 mRNA by EBV infection. We performed real-time RT-PCR to analyse the changes of STMN1 mRNA in resting B cells and 1 or 7 days post-EBV-infected B cells. Resting B cells were infected with EBV. Following 2 h incubation at 37 °C, the same volume of complete medium containing cyclosporin A (0.5 μg/ml) was added. After the cultures were incubated for 1 or 7 days, the level of the STMN1 mRNA was analysed.

Change of cell cycle and cell growth parameters

We investigated changes of cell cycle parameters in resting B cells, in day 1 or 7 days post-EBV infection and in LCL. We first analysed components of the cell cycles of resting B cells and the corresponding LCL using PI staining. Resting B cells mostly accumulated in the $G_0 + G_1$ phases of the cell cycle (Fig. 5a). However, LCL transformation induced an increase in the percentage of cells in the S-phase and a reduction in the percentage of cells in $G_0 + G_1$ (Fig. 5a). Next, we analysed effects of EBV infection on the cell cycle profile of resting B cells. EBV infection lead to an increase in the percentage of cells in the S-phase of the cell cycle and a reduction in the percentage of cells in the $G_0 + G_1$ phase compare to the cell cycles of resting B cells (Fig. 5b). We investigated changes in cell population growth using a cell proliferation assay for resting B cells and 1 or 7 days post-EBV infection. The increase in cell population growth was observed at 7 days post-infection compared to that of resting B cells (Fig. 5c).

DISCUSSION

The Epstein–Barr virus infects resting B cells and transforms them into proliferating LCL *in vitro* by changing the cellular gene expression through expression of essential viral genes. Although resting B cells are mortal, LCLs have long been believed to be immortal (Sugimoto *et al*. 2004). In this study, we have shown that LCLs changed the expression of a number of genes that were involved in cellular metabolism and proliferation. In LCLs, there was also up-regulated or down-regulated expression of many genes involved in the cell cycle, immune response, regulation of transcription, signal transduction and proteolysis. LCLs usually have normal diploid karyotypes (Sugimoto *et al*. 2004). However, through microarray analysis, we were able to observe changes of many cell cycle-related genes in the LCLs. The proto-oncogene *c-Myc*, which is a direct target gene of EBNA2, is a potent activator of cell proliferation in B cells (Kaiser *et al*. 1999; Pajic *et al*. 2000). Myc triggers cell proliferation in a human EBV-EBNA1 positive B-cell line, P493-6, by promoting the expression of a set of cell cycle activators

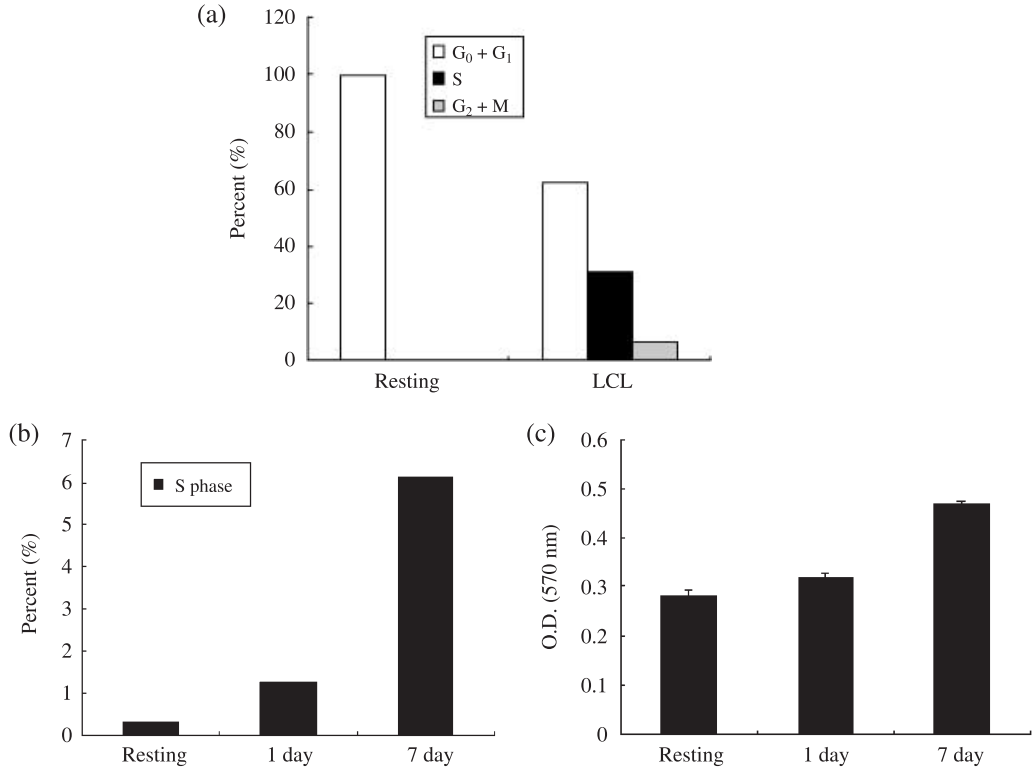

Figure 5. Changes of cell cycle and cell growth by EBV infection. We investigated changes in cell cycle progression between resting B cells and LCL by FACS analysis of propidium iodide-stained cells (a). The percentage of cells in the S-phase of the cell cycle was analysed in resting and 1 or 7 days post-EBV infection (b). We analysed changes in cell population growth using Cell Proliferation Assay (Promega) in resting B cells and 1 or 7 days post-EBV-infected B cells (c).

(Pajic *et al*. 2000). Among the 343 EBV-induced genes, 14 were involved in cell cycle progression. *CDK2*, *STMN1*, *CDC2*, *STK6*, *CCNA2*, *CCNG1*, *CDK4*, *CINP*, *PRC1*, *YWHAG* and *ACTB* were up-regulated, and *DUSP1*, *CLK1* and *CCNL1* were down-regulated in LCL. In previous studies, the *CDK2*, *CDK4* and *CDC2* genes were known to have been EBV-induced (Pajic *et al*. 2000; O'Nions & Allday 2003). These three genes are all involved in the mitotic cell cycle. Apart from these, 11 genes have been newly identified in this study. It is characteristic of LCLs that the expression level of cell cycle-related genes is changed, suggesting substantially higher proliferation activity of LCLs compared to resting B cells. The cell cycle of LCLs is regulated at either the G_1/S or G_2/M boundaries, depending on p53 concentration (Chen *et al*. 1998). In a previous study, *LMP1* expression was able to up-regulate the transcription of cyclin D1 via the nuclear factor-κB signalling pathway, promoting the transition from G_1 to S, leading to the cell entering S-phase prematurely (Deng *et al*. 2003). In this study, the LCL cohort showed increased percentage of cells in the S-phase of the cell cycle compare to the resting B cells. Thus, cell cycle-related genes identified by our microarray analysis may play a role in cell cycle progression of LCLs.

Among the 11 newly identified genes, it is known that *STMN1* plays a role in regulation of the cell cycle (Liedtke *et al*. 2002; Rubin & Atweh 2004; Liu *et al*. 2005). It has previously been

reported that *STMN1* level is elevated in various tumour cells, such as hepatocellular carcinoma and adenoid cystic carcinoma of salivary glands (Li *et al*. 2005; Nakashima *et al*. 2006). STMN1 is a microtubule-destabilizing phosphoprotein that plays a critical role in regulation of mitosis (Mistry & Atweh 2001). When STMN1 is phosphorylated by cdc2, its microtubule-depolymerizing activity is lost and the mitotic spindle is formed (Mistry & Atweh 2001). However, dephosphorylation of STMN1 plays a critical role in regulation of exit from mitosis (Mistry & Atweh 2001). In addition, forced expression of STMN1 has resulted in the arrest of cells in the early stages of mitosis, and inhibition of STMN1 has resulted in accumulation of cells in the G_2 + M phases (Rubin & Atweh 2004; Liu *et al*. 2005). Thus, regulation of STMN1 expression is important for cell cycle progression. In this study, both the level of STMN1 mRNA and the percentage of cells in the S-phase of the cell cycle were shown to be increased not only LCL, but also in the 7-day post-infection B cells, compared to resting B cells. Therefore, we suppose that STMN1 plays a role not only in progression of the cell cycle in EBV-transformed LCL, but also in the initiation of the cell cycle progression in EBV-infected B cells. However, there is a difference in over-expressed STMN1 mRNA level between 7-day post-EBV-infected cells and LCL (Figs 3a and 4). STMN1 mRNA level was higher in 7-day post-EBV infection than in LCL compared to each resting B cell. There is a need to investigate whether the difference of over-expressed STMN1 mRNA level induces differences in cell cycle progression and cell population growth.

It has been reported that the EBV genome was integrated at intron1 of the *BACH2* gene located on chromosome 6q15 of the human genome in the Raji cell line, which was established from BL tissue (Takakuwa *et al*. 2004). *BACH2* was also not expressed in the Raji cell line (Takakuwa *et al*. 2004). In this study, microarray and real-time RT-PCR analyses revealed that expression of the *BACH2* was considerably reduced in LCLs compared to resting B cells. However, it has not yet been reported whether the EBV genome was integrated in the region of the *BACH2* gene involved in the human genome of LCLs. EBV could be an aetiological factor in lymphoma development, through not only the expression of both EBV genes and host genes, but also by the integration of the virus genome into the host chromosome. Therefore, it needs to be investigated whether the EBV genome was integrated in the region of *BACH2* in LCLs.

According to the results of the microarray analysis, *STMN1*, *RAB9A*, *RAB27A* and *MYBL2* were up-regulated, while *RAB37*, *JUNB* and *VAV3* were down-regulated in the LCLs. Among the seven EBV-changed oncogenes, three genes were involved in the *Rab* family. The human genome is predicted to contain 60 *RAB* genes, suggesting that future work could reveal further links between *Rab* dysfunction and disease (Seabra *et al*. 2002). Mutations in *Rab27a* result in Griscelli syndrome, caused by defects in melanosome transport in melanocytes and loss of cytotoxic killing activity in T cells (Seabra *et al*. 2002). In infectious diseases caused by intracellular microorganisms, the function of endocytic *Rab*s is altered either as part of host defence or as part of the survival strategy of the pathogen (Seabra *et al*. 2002). Ras-like GTPases of the Rab family play a role as regulators of myosin function in secretory vesicles, mitochondria, mammalian melanosomes and endosome transport (Seabra & Coudrier 2004). Cytokines such as tumour necrosis factor-α, granulocyte colony-stimulating factor, lymphotoxin and lymphotoxin-β have been found to be regulated by EBV infection (Spender *et al*. 2002). Recent data have shown that the exogenous expression of the dominant active mutant of *Rab27A* reduces antigen-induced histamine release from the rat basophilic leukaemia cell, RBL-2H3. Thus, we have inferred that these Rab family members might be related to functions of exocytosis of lysosomes and granules released with various cytokines containing histamine.

In conclusion, we have shown that LCLs had characteristic properties of EBV latency group III and had a distinct cellular gene expression profile representing the signature of high cell

proliferation activity and changes in progression through the cell cycle. In addition, this study has suggested that *STMN1* induced by EBV might play roles in cell cycle progression and proliferation in human B lymphocytes.

ACKNOWLEDGEMENTS

This work was supported by an intramural grant from National Genome Center, National Institute of Health, Center for Disease Control and Prevention, Seoul, Korea. We thank Dr. Adam Turner for editing of this manuscript.

REFERENCES

Al Saati T, Delecluze HJ, Chittal S, Brousset P, Magaud JP, Dastugue N, Cohen-Knafo E, Laurent G, Rubin B, Delsol G (1992) A novel human lymphoma cell line (Deglis) with dual B/T phenotype and gene rearrangements and containing Epstein-Barr virus genomes. *Blood* **80**, 209–216.

Bornkamm GW, Hammerschmidt W (2001) Molecular virology of Epstein-Barr virus. *Philos. Trans. R. Soc. Lond. B. Biol. Sci*. **356**, 437–459.

Carter KL, Cahir-McFarland E, Kieff E (2002) Epstein-Barr virus-induced changes in B-lymphocyte gene expression. *J. Virol*. **76**, 10427–10436.

Chen W, Huang S, Cooper NR (1998) Levels of p53 in Epstein-Barr virus-infected cells determine cell fate: apoptosis, cell cycle arrest at the G1/S boundary without apoptosis, cell cycle arrest at the G2/M boundary without apoptosis, or unrestricted proliferation. *Virology* **251**, 217–226.

Cohen JH, Fischer E, Kazatchkine MD, Lenoir GM, Lefevre-Delvincourt C, Revillard JP (1987) Expression of CR1 and CR2 complement receptors following Epstein-Barr virus infection of Burkitt's lymphoma cell lines. *Scand. J. Immunol*. **25**, 587–598.

Deng L, Yang J, Zhao XR, Deng XY, Zeng L, Gu HH, Tang M, Cao Y (2003) Cells in G2/M phase increased in human nasopharyngeal carcinoma cell line by EBV-LMP1 through activation of NF-kappaB and AP-1. *Cell Res*. **13**, 187–194.

Farrell PJ, Allan GJ, Shanahan F, Vousden KH, Crook T (1991) p53 is frequently mutated in Burkitt's lymphoma cell lines. *EMBO J*. **10**, 2879–2887.

Kaiser C, Laux G, Eick D, Jochner N, Bornkamm GW, Kempkes B (1999) The proto-oncogene c-myc is a direct target gene of Epstein-Barr virus nuclear antigen 2. *J. Virol*. **73**, 4481–4484.

Koppel J, Boutterin MC, Doye V, Peyro-Saint-Paul H, Sobel A (1990) Developmental tissue expression and phylogenetic conservation of STMN1, a phosphoprotein associated with cell regulations. *J. Biol. Chem*. **265**, 3703–3707.

Li C, Tan YX, Zhou H, Ding SJ, Li SJ, Ma DJ, Man XB, Hong Y, Zhang L, Li L, Xia QC, Wu JR, Wang HY, Zeng R (2005) Proteomic analysis of hepatitis B virus-associated hepatocellular carcinoma: identification of potential tumor markers. *Proteomics* **5**, 1125–1139.

Liedtke W, Leman EE, Fyffe RE, Raine CS, Schubart UK (2002) Stathmin-deficient mice develop an age-dependent axonopathy of the central and peripheral nervous systems. *Am. J. Pathol*. **160**, 469–480.

Liu A, Stadelmann C, Moscarello M, Bruck W, Sobel A, Mastronardi FG, Casaccia-Bonnefil P (2005) Expression of stathmin, a developmentally controlled cytoskeleton-regulating molecule, in demyelinating disorders. *J. Neurosci*. **25**, 737–747.

Mistry SJ, Atweh GF (2001) Stathmin inhibition enhances okadaic acid-induced mitotic arrest: a potential role for stathmin in mitotic exit. *J. Biol. Chem*. **276**, 31209–31215.

Nakashima D, Uzawa K, Kasamatsu A, Koike H, Endo Y, Saito K, Hashitani S, Numata T, Urade M, Tanzawa H (2006) Protein expression profiling identifies maspin and stathmin as potential biomarkers of adenoid cystic carcinoma of the salivary glands. *Int. J. Cancer* **118**, 704–713.

Neitzel H (1986) A routine method for the establishment of permanent growing lymphoblastoid cell lines. *Hum. Genet*. **73**, 320–326.

O'Nions J, Allday MJ (2003) Epstein-Barr virus can inhibit genotoxin-induced G1 arrest downstream of p53 by preventing the inactivation of CDK2. *Oncogene* **22**, 7181–7191.

Pajic A, Spitkovsky D, Christoph B, Kempkes B, Schuhmacher M, Staege MS, Brielmeier M, Ellwart J, Kohlhuber F, Bornkamm GW, Polack A, Eick D (2000) Cell cycle activation by c-myc in a burkitt lymphoma model cell line. *Int. J. Cancer* **87**, 787–793.

Pelloquin F, Lamelin JP, Lenoir GM (1986) Human B lymphocytes immortalization by Epstein-Barr virus in the presence of cyclosporine A. *In Vitro Cell. Dev. Biol.* **22**, 689–699.

Rubin CI, Atweh GF (2004) The role of stathmin in the regulation of the cell cycle. *J. Cell Biochem.* **93**, 242–250.

Seabra MC, Coudrier E (2004) Rab GTPases and myosin motors in organelle motility. *Traffic* **5**, 393–399.

Seabra MC, Mules EH, Hume AN (2002) Rab GTPases, intracellular traffic and disease. *Trends Mol. Med.* **8**, 23–30.

Shimada K, Uzawa K, Kato M, Endo Y, Shiiba M, Bukawa H, Yokoe H, Seki N, Tanzawa H (2005) Aberrant expression of RAB1A in human tongue cancer. *Br. J. Cancer* **92**, 1915–1921.

Spender LC, Cornish GH, Sullivan A, Farrell PJ (2002) Expression of transcription factor AML-2 (RUNX3, CBF (alpha)-3) is induced by Epstein-Barr virus EBNA-2 and correlates with the B-cell activation phenotype. *J. Virol.* **76**, 4919–4929.

Sugimoto M, Tahara H, Ide T, Furuichi Y (2004) Steps involved in immortalization and tumorigenesis in human B-lymphoblastoid cell lines transformed by Epstein-Barr virus. *Cancer Res.* **64**, 3361–3364.

Takakuwa T, Luo WJ, Ham MF, Sakane-Ishikawa F, Wada N, Aozasa A (2004) Integration of Epstein-Barr virus into chromosome 6q15 of Burkitt lymphoma cell line (Raji) induces loss of BACH2 expression. *Am. J. Pathol.* **164**, 967–974.

Tsurumi T, Fujita M, Kudoh A (2005) Latent and lytic Epstein-Barr virus replication strategies. *Rev. Med. Virol.* **15**, 3–15.